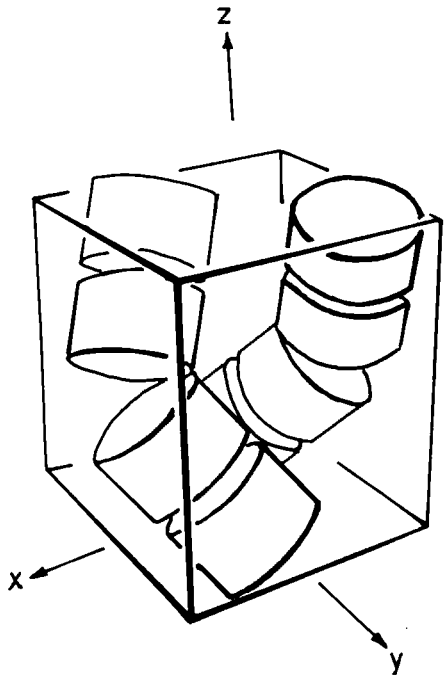


FIGURE 4 Schematic drawing of the protein arrangement in the unit cell obtained from model fits to the $H_2O$ data at 50 Å resolution.

hydrodynamic measurements (M. Zulauf, unpublished data). While the former shows the channel structure in detail, the latter permit estimation of the outer dimensions of the protein and suggest that the trimer is roughly of cylindrical shape with a diameter of 76 Å and a height of 38 Å. We have therefore started to analyze the $H_2O$ data with the model sketched in Materials and Methods. The final aim of the analysis is to find a structural model for the protein and the detergent with a satisfactory *R*-factor in all contrasts, where only the densities vary from one contrast to the other, allowing identification and localization of the corresponding moiety.

At 50 Å resolution the $H_2O$ data can be modeled well with a single cylinder for the trimer. The dimer of trimers in the asymmetric unit consists of a coaxial arrangement of two cylinders, and the gross protein arrangement in the unit cell is shown in Fig. 4: four dimers wind in a double helical way around the $4_2$-axis (*z*-axis). The orientation angles of the dimer axis are virtually identical to those of the noncrystallographic threefold axis found from x-ray data by rotation function analysis at 10 Å resolution (R. Karlson, private communication).

At 16 Å resolution, more details are needed to model the $H_2O$ data, some of which confirm structural details as observed by electron microscopy (EM): the two protein trimers in the dimer are mirror images of each other, and the spacing is achieved by three protein feet in register. Two sets of threefold indentations near the protein mantle render the surface more irregular. Three channels starting at the outside extend into the protein body and eventually merge towards the inside; their diameter is, however, smaller than expected from the EM reconstitutions. In addition, several further structures outside the protein body and not obeying threefold symmetry have to be introduced in the model. These pertain to detergent, which fills lateral gaps between the protein. At this resolution, the starting model describes the $H_2O$ data with an *R* factor of 0.35. Comparison of Fourier maps involving calculated and observed amplitudes will be used to refine the model further.

*Received for publication 3 May 1985.*

## REFERENCES

1. Rosenbusch, J. P. 1974. Characterization of the major envelope protein from *Escherichia coli*. *J. Biol. Chem.* 249:8019–8029.
2. Garavito, R. M., and J. P. Rosenbusch. 1980. Three-dimensional crystals of an integral membrane protein: An initial x-ray analysis. *J. Cell Biol.* 86:327–329.
3. Garavito, R. M., J. A. Jenkins, J. N. Jansonius, R. Karlson, and J. P. Rosenbusch. 1983. X-ray diffraction analysis of matrix porin, an integral membrane protein from *Escherichia coli* outer membrane. *J. Mol. Biol.* 164:313–327.
4. Roth, M., A. Lewit-Bentley, and G. A. Bentley. 1984. Scaling and phase-difference determination in solvent contrast variation experiments. *J. Appl. Cryst.* 17:77–84.
5. Dorset, D. L., A. Engel, M. Haener, A. Massalski, and J. P. Rosenbusch. 1983. Two-dimensional crystal packing of matrix porin. *J. Mol. Biol.* 165:701–710.

# DIFFUSE SCATTERING PROBLEM IN MEMBRANE DIFFRACTION

## A Solution

C. R. WORTHINGTON
*Carnegie-Mellon University, Pittsburgh, Pennsylvania 15213*

The disorder parameters inherent in the x-ray diffraftion data from multi-layered membrane-pair assemblies have been studied. The assemblies may contain both lattice disorder and positional disorder. Lattice disorder refers to variation in the width of the unit cell and it gives rise to the broadening of the reflections. Swollen nerve myelin is the



BIOPHYS. J. © Biophysical Society · 0006–3495/86/01/98/04 $1.00
Volume 49 January 1986 98–101

classic example (1). The correct procedure (2) for measuring the integrated intensities of these broadened reflections was given in 1974. Thus lattice disorder poses no problems for x-ray structure analysis. Positional disorder is not so straightforward. It is caused by variation in the separation of the two membranes comprising the membrane pair and gives rise to diffuse scatter that is superimposed on the x-ray data. The diffuse scattering problem refers to the difficulty in evaluating and removing the diffuse scattering component so that the undistorted x-ray data is obtained. A solution to this problem is described.

In previous work on the effects of disorder in membrane diffraction, intensity formulas (3–5) were derived for two different lattice models. The estimates on the size of the positional disorder (3–5) were surprisingly large, and this tended to emphasize possible errors in data processing. There was confusion on the consequences of these disorders: it was stated or implied (3, 4) that past x-ray work that neglected these effects was either inconclusive or wrong. However, before discarding all previous work on membranes it might be wise to reexamine the significance of the effects. Lattice disorder is of no concern provided that the correct procedure (2) is used. Positional disorder is, however, of direct concern: before 1975 this disorder was uniformly neglected (as a second-order effect). Thus we have only to treat positional disorder.

## THEORY

The intensity trace from the densitometer (or detector) is $\mathbf{I}_{TR}(X)$ and results from convoluting the intensity profile $\mathbf{I}_{OBS}(X)$ with the x-ray beam and the densitometer slit. If the assembly contains no positional disorder then

$$\mathbf{I}_{OBS}(X) = J(X)L(X), \tag{1}$$

where $J(X)$ is the undistorted intensity transform and $L(X)$ is the interference function of the lattice. On the other hand, when positional disorder is present

$$\mathbf{I}_{OBS}(X) = J_{DIS}(X)L(X) + \Delta\mathbf{I}(X), \tag{2}$$

where $J_{DIS}(X)$ is the disordered intensity transform and $\Delta\mathbf{I}(X)$ is a correction term. The two terms: $J_{DIS}(X)$ and $\Delta\mathbf{I}(X)$ are dependent on the lattice model. The form of $J_{DIS}(X)$ is, however, invariant.

Let the membrane at $x = \eta$ have electron density $m(x)$ and Fourier transform $M(X) = A(X) + iB(X)$. The intensity transform is $J(X)$ and $J(X) = S(X) + D(X)$, where $S(X)$ is the sum of the squares of $D(X)$ is the corresponding interference term. A simple lattice model for disorder is as follows: starting at $x = 0$, roll gaussian dice for $x = d$, roll again for the location of the membrane center at $x = -\eta$ and the same dice for its pair at $x = \eta$ and so on. The disordered intensity transform $J_{DIS}(X)$ is given by

$$J_{DIS}(X) = S(X) + H(X)D(X), \tag{3}$$

where $H(X) = e^{-2(\pi cX)^2}$ and where $c$ is the positional disorder parameter. Thus positional disorder reduces the interference term.

We choose to express $J_{DIS}(X)$ in unconventional form:

$$J_{DIS}(X) = J(X) + DSC(X), \tag{4}$$

where $DSC(X)$ is the diffuse scattering component superimposed on the undistorted intensity transform and where $DSC(X) = -\{(1 - H(X)\}D(X)$. Note that $DSC(X)$ can be negative but $J_{DIS}(X)$ remains positive. The correction term $\Delta\mathbf{I}(X)$ for the above model is

$$\Delta\mathbf{I}(X) = S(X)\{1 - H(X)\}\{N - L(X)\}, \tag{5}$$

where the assembly contains $N$ lattice points. The correction term is dependent on the lattice disorder via $L(X)$ and positional disorder via $H(X)$. For moderate lattice disorder and for large values of $X$, the interference function $L(X)$ approximates to $N$ so that the correction term vanishes.

## EXPERIMENT

A set of integrated intensities $\mathbf{I}(h)$ is obtained by measuring the area under the $\mathbf{I}_{TR}(X)$ curve after the background scattering curve has been subtracted. The measured $\mathbf{I}(h)$ contain information on $DSC(h)$, the diffuse scattering component.

We note three observations relating to experiment: (*a*) the $DSC(h)$ component is contained within the $\mathbf{I}(h)$ values; (*b*) the $\Delta\mathbf{I}(X)$ values do not contribute to the $\mathbf{I}(h)$ values; and (*c*) the background scattering curve is relatively unaffected by both the $DSC$ and $\Delta\mathbf{I}$ terms.

These three observations have been verified by calculation. The $\mathbf{I}_{TR}(X)$ curve for rod outer segment (*ROS*) membranes is shown in Fig. 1. The $X$-range includes the diffraction orders $h$ = 6–8. The overlap between orders derives entirely from the lattice disorder. The lattice disorder was simulated by a paracrystalline lattice with $d$ = 296 Å, $N$ = 30 and $\Delta$ = 9.8 Å, where $\Delta$ is the rms value of the gaussian function (6). The $DSC$ component (assuming $c$ = 5.1 Å) is also shown in Fig. 1. The $DSC$ component increases $\mathbf{I}(6)$ but decreases the $\mathbf{I}(7)$ value. The $\Delta\mathbf{I}$ values are not shown for after integration over each reflection they tend to zero because each integral over $L(X)$ is equal to $N$.

## ANALYSIS

A set of phases is assumed. The electron density of the membrane pair is computed using $C(h)$ as the Fourier

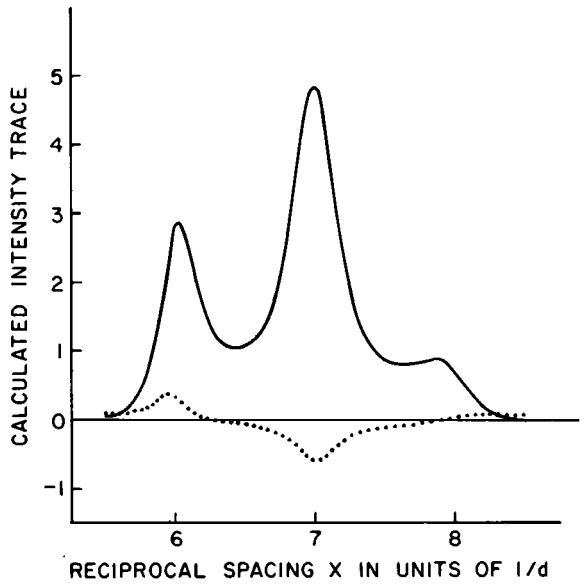


FIGURE 1 The calculated $\mathbf{I}_{TR}(X)$ curve (—) for a model *ROS* membrane structure as a function of the reciprocal spacing $X$, in units of $1/d$. The diffraction orders $h$ = 6 – 8 are shown. The overlap between orders arises from the lattice disorder ($\Delta$ = 9.8 Å, $N$ = 30, and $d$ = 296 Å). The $DSC$ component (---) was calculated using a positional disorder of $c$ = 5.1 Å. The effect of the $DSC$ component is to either increase or decrease the observed integrated intensities.

coefficients. We begin with $C(h) = [\mathbf{I}(h)]^{1/2}$. Fourier transformation of the membrane profile about its center provides a set of calculated As and Bs and hence a set of Ss and Ds. If $J_{CALC} = S_{CALC} + D_{CALC}$ matches the $\mathbf{I}(h)$ values then $c = 0$ and there is no positional disorder. This is a sensitive test. If, however, the $J_{CALC}$ and $\mathbf{I}(h)$ values do not match then $c > 0$ and the problem is to find the correct $c$ value. Our procedure is to run a series of values for $c$ say $c$-test in the next cycle and then to choose an optimum value for $c$. The Fourier coefficients for this cycle are $C(h) = [\mathbf{I}(h) + \{1 - H(X)D(X)\}]^{1/2}$, where $H(X)$ contains $c$-test. The iteration continues until the correct $c$ value is recovered. This procedure has been verified using model x-ray data (7).

## RESULTS

X-ray diffraction data from normal and swollen nerve myelin and from *ROS* membranes have been analyzed for positional disorder and the $c$ parameters have been determined. The x-ray data and phases used in the analysis are as follows:

Nerve myelin (2): frog sciatic nerve $d = 171$ Å, $h = 9$ orders and the phases $(-1, +1, +1, -1, -1, +1, -1, -1, -1)$.

Swollen nerve (2): frog sciatic nerve swollen in 6.5% glycerol $d = 224$ Å, $h = 12$ and phases $(-1, +1, +1, +1, -1, -1, -1, -1, -1, -1, -1, -1)$.

ROS membranes (8): frog retina $d = 296$ Å, $h = 11$ and phases $(+1, +1, +1, +1, +1, -1, -1, -1, +1, +1, +1)$.

The lattice disorder was obtained from an experimental study of the line broadening of the *ROS* diffraction (8) and of the nerve myelin patterns (unpublished data). The estimate of $\Delta$, the rms value of the paracrystalline gaussian function (6) was obtained using either a gaussian or Cauchy analysis.

A comparison of our disorder parameters with those quoted in the literature is presented in Table I. The disorder parameters are quoted in terms of the rms values of the appropriate gaussian functions.

Our results on positional disorder were decidedly unexpected and they are in drastic disagreement with previous estimates (3–5, 9) (see Table I). Even though typical densitometer traces of membranes (2, 10) gave little or no support for the precense of positional disorder, it was a surprise that positional disorder in nerve myelin and in *ROS* membranes was almost nonexistent.

Our results on lattice disorder are in fair agreement with previous results on nerve myelin and *ROS* membranes although our patterns show somewhat less disorder. The large lattice disorders for swollen nerve (4, 5) in Table I are puzzling. Unfortunately, the x-ray patterns with these large lattice disorders were not shown. On the other hand, x-ray patterns of swollen nerve (1, 11) and a densitometer trace (2) are in the literature. For example, Fig. 1 of reference 1 and Fig. 1 *B* of reference 11 both show $h = 7$ or 8 orders of $d = 250$ Å and these patterns are consistent with our measurement of $\Delta = 5.5$ Å.

TABLE I
DISORDER PARAMETERS $\Delta$ AND $c$ FOR THREE MEMBRANE STRUCTURES

| | $\Delta$ in Å | $c$ in Å | Reference |
|---|---|---|---|
| Nerve Myelin: | 5.2 | 4.0 | [4] |
| | 1.8 | 1.5 | [5] |
| | 3.0 | 0.0 | This Study |
| Swollen Nerve: | 12.3 | 6.2 | [4] |
| | 30.0 | 8.0 | [5] |
| | 5.5 | 0.0 | This Study |
| ROS Membranes: | 13.4 | 5.7 | [3] |
| | 13.6 | 5.1 | [9] |
| | 9.8 | 1.0 | This Study |

## DISCUSSION

The three membrane assemblies so far studied contain lattice disorder but very little if any positional disorder. The conclusion that these structures contain very little positional disorder restores the validity of x-ray work before 1975 wherein positional disorder was uniformly neglected (as a second-order effect). In particular, the above conclusion also validates the results of the swelling method as applied to nerve myelin (2) contrary to a negative claim by Nelander and Blaurock (4).

The correctness of our analysis of positional disorder has been verified using model x-ray data (7) and it has been shown that our method is quite sensitive in detecting small amounts of positional disorder. Future work centers on the dependence of the $c$ parameter on the phase choice and on the number of orders used in the analysis.

*Received for publication 30 April 1985.*

## REFERENCES

1. Worthingotn, C. R., and A. E. Blaurock. 1969. A low-angle study of the swelling behavior of peripheral nerve myelin. *Biochim. Biophys. Acta.* 173:427–435.
2. Worthington, C. R., and T. J. McIntosh. 1974. Direct determination of the lamellar structure of peripheral nerve myelin at moderate resolution (7 Å). *Biophys. J.* 14:703–729.
3. Schwartz, S., J. E. Cain, E. A. Dratz, and J. K. Blasie. 1975. An analysis of lamellar x-ray diffraction from disordered membrane multilayers with application to data from retinal rod outer segments. *Biophys. J.* 15:1201–1233.
4. Nelander, J. C., and A. E. Blaurock. 1978. Disorder in nerve myelin: phasing the higher order reflections by means of diffuse scatter. *J. Mol. Biol.* 118:497–532.
5. Gbordzoe, M. K., and W. Kreutz. 1978. Direct determination of the electron-density profile at the nerve myelin membrane with paracrystalline lattice distortions taken into account. *J. Appl. Cryst.* 11:489–495.
6. Hosemann, R., and S. N. Bagchi. 1962. Direct Analysis of Diffraction by Matter. Elsevier/North-Holland, Amsterdam.
7. Worthington, C. R., and Mita Gupta. 1985. Direct determination of the substitution disorder parameter in membrane diffraction. *Biophys. J.* 47(2, Pt. 2:363*a*. (Abstr.)

8. Worthington, C. R. 1981. The lamellar structure of intact vertebrate retinal photoreceptors: a verification of phases. *Photobiochem. Photobiophys.* 3:43–51.
9. Funk, J., W. Welte, N. Hodapp, I. Wutschel, and W. Kreutz. 1981. Evaluation of the electron density profile of the frog rod outer segment disc-membrane in vivo using x-ray diffraction. *Biochim. Biophys. Acta.* 640:142–158.
10. Akers, C. K., and D. F. Parsons. 1970. X-ray diffraction of myelin membrane. I. Optimal conditions for obtaining unmodified small angle diffraction data from frog sciatic nerve. *Biophys. J.* 10:101–115.
11. McIntosh, T. J., and C. R. Worthington. 1974. Direct determination of the lamellar structure of peripheral nerve myelin at low resolution (17 Å). *Biophys. J.* 14:363–386.

# ORIENTATION OF THE PRIMARY DONOR IN ISOLATED PHOTOSYSTEM II REACTION CENTERS STUDIED BY ELECTRON PARAMAGNETIC RESONANCE

A. W. RUTHERFORD AND S. ACKER
*Service de Biophysique, Département de Biologie, Centre d'Etudes Nucléaires de Saclay, 91191 Gif-sur-Yvette, France*

Isolated photosystem II (PS II) reaction center complexes were partially dried on polyester (mylar) sheets. Using electron paramagnetic resonance (EPR) measurements of the cytochrome $b_{559}$ that is present in the PS II reaction center, we found that the isolated complexes were oriented on the mylar with the same geometry as that shown when oriented in the natural membrane. From the orientation dependence of the EPR signal from $^3$P680, the triplet state of the primary donor chlorophyll, we concluded that the plane of the chlorophyll macrocycle was oriented parallel to the mylar sheet and therefore parallel to the plane of the natural membrane. This is different from the situation in purple bacteria where the analogous primary bacteriochlorophyll donor is perpendicular to the membrane plane.

## RESULTS

PS II reaction center complexes were isolated from spinach chloroplast membranes as described previously (1). The isolated reaction centers were painted onto mylar sheets and dried in a 90% humidity argon atmosphere for 48 h at 4°C in darkness. EPR spectra of the dried films showed signals characteristic of cytochrome $b_{559}$ in its low potential oxidized form. Fig. 1 shows that the two low-spin haem signals ($gz = 2.97$, $gy = 2.2$) were orthogonal, with the $gz$ signal being maximum when the mylar sheet was parallel to the magnetic field. This orientation dependence is the same as that found for this cytochrome in oriented membrane preparations and has been interpreted previously as indicating that the haem plane is perpendicular to the membrane plane (reviewed in reference 2). We therefore concluded that, after being dried, the isolated reaction center complexes become ordered in two dimensions with the same geometry as in the native membrane. This may be due to the alignment of adjacent hydrophobic and hydrophyllic regions of these membrane-spanning, intrinsic proteins.

When the isolated PS II reaction centers were reduced with sodium dithionite in darkness, an EPR signal at g 2.0045, ($\Delta H \simeq 9$ G) was induced. This signal is attributed to the semiquinone form of the primary plastoquinone acceptor, $Q_A$, in the absence of the characteristic interaction with iron (reviewed in reference 2). This signal showed little anisotropy.

When reduced PS II reaction centers are illuminated at low temperature, the following photochemistry takes place:

$$P680\ Ph\ Q_A^- \xrightarrow{light} P680^+\ Ph^-\ Q_A^- \longrightarrow {}^3P680\ Ph\ Q_A^-,$$

where Ph is pheophytin, the primary electron acceptor and $^3$P680 is the unusual spin-polarized triplet state of P680 formed by recombination of the radical pair, $P680^+\ Ph^-$.

$^3$P680 was detected by EPR in the oriented PS II reaction centers (Fig. 2). The $^3$P680 signal was orientation dependent with the outer $Z$ peaks showing clear maxima when the mylar was perpendicular to the magnetic field, while the $X$ and $Y$ peaks showed less well-marked maxima when the mylar was parallel to the magnetic field. The $Z$ peak is associated with the axis perpendicular to the chlorophyll macrocycle (3). Thus the plane of the chlorophyll macrocycle is parallel to the mylar sheet. The data on the cytochrome showed that the isolated reaction centers were oriented on the mylar with the same geometry as in the native membrane. Therefore it is concluded that the plane of the chlorophyll macrocycle of $^3$P680 is oriented parallel to the plane of membrane. This agrees with the conclusion obtained from similar but less well-resolved data using oriented PS II membranes. (2).

This conclusion is of interest in two respects. First, it indicates that the extremely rapid electron transfer reaction between P680 and Ph occurs between planar mole-